Characterization of Lipid Membrane Dynamics by Simulation: 3. Probing Molecular Transport Across the Phospholipid Bilayer

B. Jin[1] and A. J. Hopfinger[1,2]

Received September 26, 1996; accepted October 8, 1996

Purpose. The goal of this study is to elucidate the role of the motions of the hydrocarbon chains of a phospholipid bilayer in penetrant diffusion. Penetrant size, as well as its position in the hydrocarbon core of the lipid bilayer, has also been explored regarding impact on the diffusion rate in a phospholipid bilayer.
Method. Molecular dynamics, MD, simulations were carried out on a model dimyristoyl phosphatidylcholine (DMPC) membrane bilayer with and without methanol and propanol as penetrants. The MD trajectories were analyzed in terms of estimating time and space properties.
Results. These simulations show that torsion angle kink shifts in the hydrocarbon chains of phospholipids are natural occurrences in a bilayer assembly. The diffusion coefficients of methanol and propanol in a DMPC lipid bilayer, as calculated from the MD simulations, agree with experimental measurements. Both methanol and propanol show different diffusion rates in different regions of the hydrocarbon chain matrix of the lipid bilayer. Solute size has more impact on diffusion rate in the bilayer regions with high torsion angle order parameters, as compared to the regions with low torsion angle order parameters.
Conclusions. The simulated transport behavior suggests that a kink shift diffusion mechanism is more likely to occur in regions with high torsion angle order parameters, and a free volume transport mechanism is more likely operative in the region with low torsion angle order parameters, mainly the center core of the bilayer. A three zone diffusion model is proposed for transport of a penetrant across a bilayer.

KEY WORDS: simulation; bilayer membrane; diffusion; transport.

INTRODUCTION

Substances penetrate biological membranes in two general ways: (1) by passive diffusion and (2) through specific transport mechanisms. Most substances transport through biological membranes via passive diffusion (1). Many models have been proposed for the molecular mechanism of transport of substances (especially for water) across phospholipid bilayers based on information provided by molecular spectroscopic analysis and other techniques. These models can be summarized and classified as follows, (a) the homogeneous solubility-diffusion model; (b) the defect model; (c) free volume models; (d) the Träuble model and Haines-Liebovitch-Träuble model; and (e) theoretical models.

The Homogeneous Solubility-Diffusion View Model

This model has been proposed in somewhat different formats by Finkelstein (2), Hanai and Haydon (3), Reeves and Dowben (4) and others. Molecules such as N_2, O_2 and other molecules similar in size to water permeate through membranes at about the same rate, but slower than water. In the homogeneous solubility-diffusion model it is assumed that molecules transport through a bilayer by dissolution and diffusion in the membrane. The permeation processes are described in three steps:

1. The molecule must dissolve into the membrane
2. The molecule has to diffuse through the membrane interior and
3. The molecule must dissolve into the surrounding environment again.

The membrane interior is treated as a homogeneous phase resembling liquid alkane with well defined boundaries. This model is straightforward and works well for molecules such as N_2 and O_2. Therefore, it has been widely used to describe the permeation process of solutes across biomembranes. However, the rate of water passing through a bilayer is much faster than expected when compared to N_2, O_2 etc.. The homogeneous solubility-diffusion model does not satisfactorily explain this observation.

The Defect Model

This model was developed by Carruthers and Melchior (5) and Deamer and Bramhall (6). Both groups found that there are at least two types of transient defects in the bilayer, which arise from thermal fluctuations, and permit solutes to cross the hydrophobic phase at different rates. The most common defect permits small neutral solutes to dissolve in the bilayer as individual molecules, then cross by diffusion processes. A second type of defect arises at the membrane-water interface. Experiments (7) show that there is a gradient of polarity decreasing toward the interior of the membrane which permits large solutes to enter the bilayer phase. Defects, such as the transient formation of a pore allowing many water molecules, and other penetrants, to pass the membrane at the same time, have also been mentioned as contributing to the permeation process.

Free Volume Models

Lieb and Stein and coworker have proposed that the membrane barrier behaves as a "soft" polymer (8–10). The bilayer interior is believed to behave as a polymer because solute permeability has a high dependence on molecular volume after being "normalized" for hydrophobicity. The solute makes a diffusive step when it is able to suddenly move from one free volume pocket to the next (also called the "hopping" mechanism). The rate of diffusion depends on the distribution of the free volume pockets as well as on the movement of the polymer matrix. Potts and Francoeur (11) have shown a direct relation between diffusion rate and number of gauche torsion angle states in the lipid tails. The presence of gauche torsion angle states disturbs an ordered, all-trans alignment of the acyl chains in a lipid bilayer, and thus, increases the amount of free volumes.

The Träuble Model and Haines-Liebovitch-Träuble Model

Träuble (12) has found that a water molecule fits neatly between the chains of two adjacent phospholipids when the

[1] Laboratory of Molecular Modeling and Design, College of Pharmacy, University of Illinois at Chicago, 833 South Wood Street M/C 781, Chicago, Illinois 60612-7231.
[2] To whom correspondence should be addressed.

0724-8741/96/1200-1786$09.50/0

chains have kinks ($g^{\mp}tg^{\mp}$). These kinks may be pictured as dynamic structural defects which represent small, mobile free volumes in the hydrocarbon phase of the membrane. Small molecules can enter into the free volumes of kinks and migrate across the membrane as part of the kinks. Thus, kinks may be regarded as intrinsic solute carriers in lipid membranes. Träuble postulates that different types of kinks having different concentrations, different free volumes and different diffusion coefficients lead to a selectivity between permeate molecules of different masses and volumes.

A model related to the kink defect model has been proposed by Haines and Liebovitch (13). This model has five features:

1. A lateral expansion of the bilayer introduces "vacancies" in the phospholipid headgroup "lattice" portion of the membrane.
2. Waters fill the vacancies as they appear.
3. An adjacent ester group in a phospholipid moves into the lattice vacancy occluding (covering) a single water molecule separating it from the bulk. The water molecule occupies a defect space created by a kink in the chain.
4. An adjacent chain adopts a kink "above" the water molecule in conjunction with its lateral headgroup jump.
5. As the water molecule, nested between the two kinks, moves "down" the two chains (toward the center of the bilayer), the chains move laterally one lattice unit.

Thus, the lateral motion of the lipid molecules is linked with water migration though the bilayer.

Theoretical Models

MD simulations have been carried out on various solutes in phospholipid bilayers. Some structural and/or transport models have been proposed based on the MD simulation results by Day and Willis (14), Nagle and Scott (15), Marcelja (16), Kjellander and Marcelja (17), McKinnon *et al.* (18), Bassolino-Klimas *et al.* (19–20) and Marrink and Berendsen (21). Day and Willis (14) calculated an upper bound for the entropy change of the membrane phase transition based on a single chain, and showed that it is less than one half the experimental entropy change of the transition. They concluded that the discrepancy with the macroscopic measure of the entropy results from the fact that the total number of single chain kink and jog ($g^{\mp}ttg^{\mp}$) defects is orders of magnitude too small.

The calculations of Nagle and Scott (15) support the notion that the thermodynamic state of a membrane is important to its functional properties. Furthermore, their results suggest that membranes, or at least parts of membranes, may exist in "near-critical states" in which fairly large-scale fluctuations in lipid density occur. They predict that such fluctuations should allow for cavity formation, and, perhaps, protein interaction and/or conformational changes. Kjellander and Marcelja (17) observed that orientational polarization propagates, in a damped oscillatory manner, more than one nanometer from each surface of the membrane.

McKinnon *et al.* (18), using nonequilibrium MD simulations, studied oxygen diffusion through a hexadecane monolayer with varying concentrations of cholesterol. They found an increased ordering of the hexadecane chains in the region of the monolayer near the added cholesterol, along with a general increase in monolayer thickness with increasing concentration of cholesterol. Calculation of diffusion coefficients suggested an enhanced diffusion rate of oxygen with added cholesterol, followed by a decrease in the diffusion coefficient at higher cholesterol concentrations.

Bassolino-Klimas *et al.* (19–20) performed a four nanosecond MD simulation of benzene diffusing through a DMPC lipid bilayer. It is the first atomic level study of solute diffusion in a lipid bilayer using an all-atom representation of a fully solvated DMPC bilayer in the L_α phase. They found that the presence of a small solute does not affect bilayer thickness, but does result in slight perturbations in the ordering of the hydrocarbon chains. Benzene molecules undergo essentially isotropic motion and rotate freely. The finding that diffusion rate is different at different positions within lipid bilayer let them to conclude that the lipid bilayer cannot be treated as a homogeneous phase. Overall, their results support a "hopping" mechanism (see the discussion of free volume models) found for the diffusion of gases through "soft" polymers.

Marrink and Berendsen (21) recently reported the MD simulation study of "a total permeation process through a lipid membrane". They conclude that the permeation of water through a lipid membrane cannot be adequately described by a simple homogenous solubility diffusion model. Both the excess free energy, and the diffusion rate, are strongly dependent on position of the penetrant in the membrane which is consistent with the inhomogeneous nature of the biomembrane. They believe the total transport process is largely determined by the free energy barrier that results from breaking interwater hydrogen bonds and the loss of favorable electrostatic interactions. The rate-limiting step is permeation through the relative rigid hydrocarbon chain region, where the resistance is highest. Marrink and Berendsen have proposed a "four-region" diffusion model, from their MD simulations.

The "four-region model" (see Fig. 1 for the bilayer locations of the four regions) consist of; Region 1: Low head group density. This region starts at the point where the presence of the membrane begins to result in a perturbation of the bulk water structure and ends where the water density and headgroup density are comparable. This region is assumed to be the least important with respect to the permeation process.

Region 2: High headgroup density. The total width of this region is about 7.5 Å. No bulk-like water is present in this region. The proposed model assumes that water diffusion takes place in this region by "hopping" from one hydration shell to another and involves the breaking and making of hydrogen bonds.

Region 3: High tail density. This region starts at the edges of the penetrating water interface and proceeds until the density of the membrane has dropped to about that of liquid hexadecane. The density of hydrocarbon chains of the phospholipids in this region is high. Almost no water molecules are present in this region. The only way to maintain favorable short-range electrostatic interactions between the membrane and the waters is provided by the carbonyl groups of the lipids. Here, the short-range force indicates the force calculated with cutoff at a distance of 8.5 Å. Due to the high lipid tail density, the overall behavior of this region of the membrane is that of an aliphatic chain fluid with high density. The permeation process in this region takes place via singly dispersed water molecules.

Region 4: Low tail density. This is the region of the midplane of the two monolayers having a width of about 11 Å.

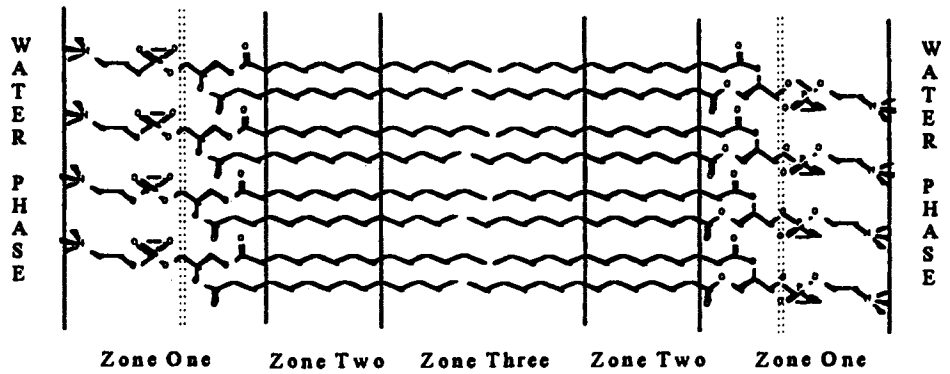

Fig. 1. The three zone diffusion model proposed from this study. The Marrink-Berendsen "Four region model" divides zone one into two regions. The boundaries between each zone are approximate.

The lipid tail density is much lower than that of Region 3. The diffusion process is assumed to be characteristic of diffusion in liquids with low viscosity, and, therefore, the diffusion rates are quite rapid.

In this paper, we, (1) discuss the natural occurrence of kink shifts in the hydrocarbon chains of a phospholipid bilayer and their role in the transport of small molecules (especially water) through a phospholipid bilayer, (2) describe the findings from MD simulations of methanol and propanol diffusion in a DMPC lipid bilayer and (3) propose a "three zone" model, and corresponding transport mechanisms, to explain solute diffusion in a lipid bilayer.

METHOD

Construction of the Simulation Model

The dimyristoyl phosphatidylcholine (DMPC) molecule was selected as the model phospholipid in this study. The structure of DMPC is shown in Fig. 2 and the corresponding torsion angles monitored in the MD simulations are defined. The DMPC structure was built using the molecular modeling package CHEMLAB II (version 11.0) (22). The aliphatic chains were assigned the trans-planar conformation. The initial geometry was optimized by the MM2 force field (23) with some force field parameters generated according to the method developed by Hopfinger and Pearlstein (24). The partial atomic charges were assigned based upon CNDO (25) calculations with some modifications made for DMPC according to the work of Stouch (26).

A DMPC bilayer was subsequently built from the DMPC molecules using available crystal data (27). The unit cell dimensions of a DMPC crystal are a = 9.5 Å, b = 10.3 Å, c = 59.0 Å and γ = 96.0° (27–28). Thirty two DMPC molecules were incorporated into a model bilayer with sixteen DMPC molecules in each monolayer.

A methanol molecule was built and energy minimized by the MM2 force field using CHEMLAB II (version 11.0). The methanol was then put into the DMPC bilayer. Four simulation models were generated with regard to the initial simulation location of the methanol, (1) a DMPC bilayer with the methanol in the headgroup region, (2) a DMPC bilayer with the methanol in the region between aliphatic chains and the headgroup, (3) a DMPC bilayer with the methanol in the region of middle aliphatic chains and (4) a DMPC bilayer with the methanol at the tail region of the aliphatic chains. The four initial MD simulation models for methanol at the different positions in the DMPC lipid bilayer are shown in Fig. 2.

In the same manner as for methanol, a propanol molecule was built and energy minimized by the MM2 force field using CHEMLAB II (version 11.0). The propanol molecule was also put into a DMPC bilayer at the same four initial simulation positions used to generate the four initial MD simulation models for methanol.

Molecular Dynamics Simulations

An atomistic MD simulation was carried out on nine molecular assemblies: one for a DMPC bilayer without a solute molecule, four for a methanol at different initial locations in a DMPC lipid bilayer and four for a propanol at different initial locations in a DMPC lipid bilayer. The MM2 force field was employed with force field extensions to include all parameters for the DMPC molecules. Explicit hydrogen atoms were included in all simulations and the MOLSIM (version 2.5) MD modeling program was employed (29).

A MD simulation was performed on the DMPC bilayer at a constant temperature of 311°K. A periodic lattice boundary condition was used (a = 37.5 Å, b = 38.5 Å, c = 60.0 Å and γ = 96.0°). The trajectory step size was 0.001 ps with a total production simulation time of 100 ps, after a 40 ps equilibration period.

Four MD simulations were performed with a methanol molecule initially positioned at the four different locations defined in Fig. 2. These diffusion simulations were also conducted at a constant temperature of 311°K. A periodic lattice boundary condition was used (a = 37.5 Å, b = 38.5 Å, c = 60.0 Å and γ = 96.0°). The trajectory step size was 0.001 ps with a total simulation time of 200 ps.

Four MD simulations were performed on the DMPC bilayer with propanol in an identical manner to the methanol MD diffusion simulations.

In all simulation modeling, high energy van der Waals interactions were removed by energy minimization using the molecular modeling package, Cerius^2 (Version 1.6) (30). The Newton-Raphson minimization method is used in Cerius^2. After the energy was minimized, the system was slowly heated to 311°K starting at 50°K at 50°K increments with 1 ps time intervals between each heating increment to allow for structural relaxation, and the distribution of the kinetic energy throughout

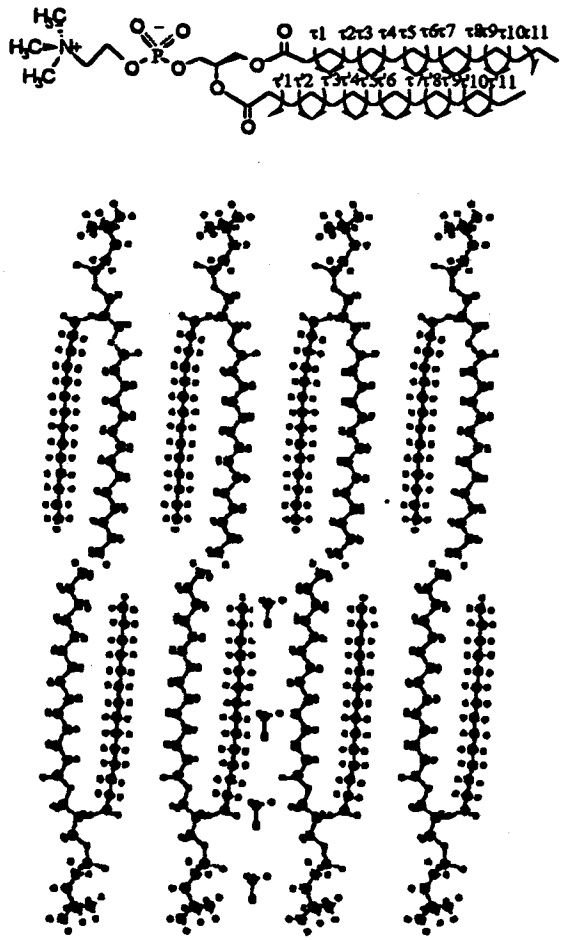

Fig. 2. The top figure is the structure of a DMPC molecule with the torsion angles investigated in this study defined. In the bottom figure is a DMPC bilayer simulation model which contains 2 × 16 DMPC molecules and one methanol molecule in the (1) head group region, (2) region between the aliphatic chains and the headgroup, (3) region of mid-region of the aliphatic chains and (4) tail region of the aliphatic chains, projected onto the a-c plane. A series of MD simulations were carried out initially placing a methanol molecule in each position one at a time.

the simulation model. The cutoff for nonbonded interactions is 8 Å.

Data Collection and Analysis

The atomic coordinates from all MD simulations were recorded in trajectory files. The corresponding sets of torsion angle trajectories were also calculated and recorded. In addition, the distance matrices of key atom pairs were calculated from the atomic coordinate trajectories.

Digital image analysis can conventionally display physical property inter-relationships. In this study, an interactive digital image analysis tool called Datascope (Version 2.1.3) (31) was used. This software allows the display of data in spreadsheet form, and as scaled and interpolated Cartesian or polar color images.

Diffusion coefficient constants were calculated from the MD trajectories. The diffusion coefficient constant may be evaluated by the (1) mean-square displacement method, or (2) by the force auto-correlation method. Both of these methods require a simulation that is long enough to arrive at a convergent value for the diffusion coefficient. In this study the mean-square displacement method was used.

RESULTS

Natural Occurrence of Kink Defects to Transport Small Molecules in a Lipid Bilayer

Potts and Francoeur (11) have studied temperature-dependent changes in water vapor permeability and the infrared absorption spectra of porcine stratum corneum (SC). They found a remarkable correlation between water permeability and the frequency of the C-H stretching vibration from the SC lipids over a broad range of temperatures. Since the spectral changes reflect a change in the number of alkyl chain gauche conformers, they concluded that water permeability is dependent upon the hydrocarbon-chain disorder of the SC lipids. They further suggested that water permeability obeys the "jump" (the free volume model) and/or "kink" propagation hypothesis (the Träuble model).

Kinks in the lipid bilayer can introduce large-scale fluctuations and generate structural defects which provide spaces for solute molecules. Although the concept that small solute molecules, like water, can diffuse through a membrane via kink shifts has been accepted in many proposed models (12–13), we are not aware of any experiment which has shown that kinks actually shift along the lipid chain. However, as part of this study we have found that kink shifts are natural spontaneous occurrences in phospholipid bilayers by using digital image analysis of our MD simulation trajectories. Figure 3 displays representations of the matrices of each of the 11 torsion angles (vertical axis) verses time (horizontal axis) of the aliphatic chains of a typical DMPC molecule from 12 ps to 56 ps of one chain in the phospholipid bilayer. The light blocks in angle-time space indicate positive deviations (>180°) from the trans state (180°); darker blocks reflect negative deviations from trans (<180°). There is a kink shift resulting from three continuous kinks with respect to the time frame shown. The first kink, (g^+tg^-), starts at 16.0 ps involving torsion angles 1, 2 and 3 (the angles were defined in Fig. 2) and ends at 24.0 ps. The second kink, (g^+tg^-), includes torsion angles 3 to 5, starts at 32.0 ps and ends at 38.4 ps. The third kink (g^-tg^+), consisting of torsion angles 5, 6 and 7, starts at 47.2 ps and ends at 49.6 ps. The speed of these kink shifts down the chain can be estimated. The projection of a C−C bond along the chain axis for the all trans state is about 1.25 Å. Therefore, the chain length from carbon 1 to carbon 7 is about 8.75 Å. Overall, the kink shift involving C_1 through C_7 starts at 16.0 ps and ends at 49.6 ps. The total time is about 33.6 ps. Thus, the rate of kink shift propagation is about 2.6×10^3 cm/s.

Many measurements have been made on passive water permeability by tritium labeling, NMR, and a variety of other techniques (2). These measured rates of permeability range from 2×10^{-4} to 20×10^{-4} cm/s. The speed at which a MD simulation kink move down a chain is much faster than the water permeability. However, we cannot reconcile these different rates because we do not know, (a) the water diffusion speeds in the headgroup and center core regions of the bilayer and (b) how

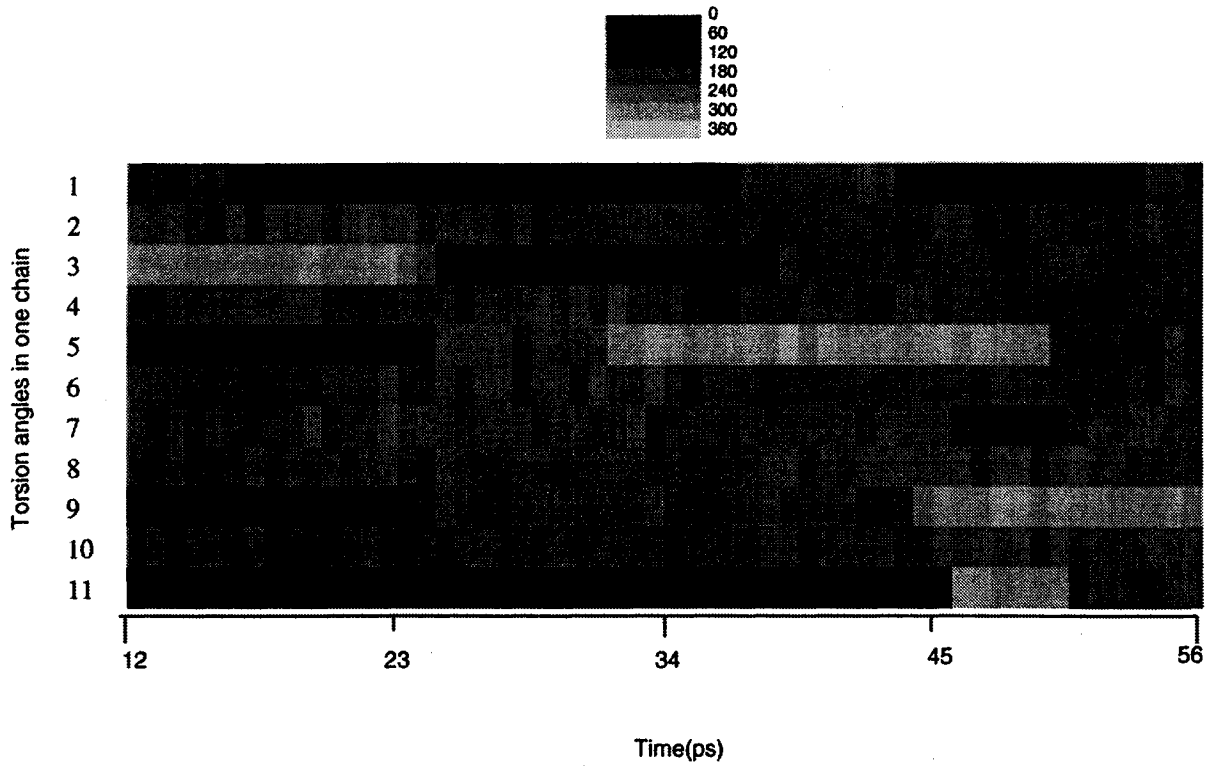

Fig. 3. Kink shifts in one typical chain torsion angle trajectory from an MD simulation.

many waters which reach the interfaces between regions are incorporated into the new diffusion mechanism, or back migrate.

It is worth pointing out that kink shifts often occur in the more ordered region of each monolayer. This is also the region of primary resistance to water transport across the membrane (32). The kinks provide free volumes for waters to nest within, and water permeation proceeds with kink shifts. The life time of a simulation kink is about 6–8 ps which agrees with a value of 7.3 ps from the work of the Berendsen group (33). The regions near the aliphatic chain tail surfaces of the two interfaced monolayers contain considerable free volume (34), and waters may (randomly) diffuse with much less resistance than in the ordered regions.

Based on the torsion angle order parameters, and other results from these MD simulation studies (35–36), and the works of other groups (19–21), we believe that water permeation through a membrane involves multiple transport mechanisms, including the processes suggested by Träuble and the free volume model by Lieb and Stein. In the relatively rigid hydrocarbon chain regions (from torsion angle 1 to torsion angle 8), waters permeate as suggested in the Träuble model. Individual water molecules can fit nicely in the spaces created by kinks as shown by Träuble. The kink shifts provide an efficient way to transport water molecules through this highly ordered (and dense) region.

In the flexible hydrocarbon chain region (torsion angle 9 in one monolayer to torsion angle 9 in the other monolayer), waters permeate more likely by the free volume mechanism. The free volume density is large in this region with relatively large free-volume pores. Therefore, it is efficient to use this mechanism for water permeation.

Calculation of the Diffusion Rates for Methanol and Propanol in a DMPC Bilayer

The different relationships between mean-square displacement (MSD) and time show different corresponding diffusion properties. The overall interdependence can be defined by,

$$\text{MSD} \propto t^n, \tag{1}$$

where the power, n, indicates different types of diffusion behavior and corresponding models:

$n = 0.5$, anomalous diffusion

$n = 1.0$, Einstein diffusion

$n = 2.0$, ballistic motion

The value of n can be calculated from plotting log (MSD) verses log (t), in which n is the slope of the plot. If the diffusion process belongs to Einstein diffusion, n should be close to one. Plots of log (MSD) verses log (t) from the MD simulations of all four initial methanol positions in a DMPC bilayer model, and the MD simulations from the four propanol positions in a DMPC bilayer model, were made. Figure 4a is a typical example of these plots. The corresponding values of n are listed in Table I. The value of n in each of the systems is above 0.9, which can be considered as 1, except for the methanol in the DMPC bilayer at position 3, and the propanol in the DMPC bilayer at position 2. The values of n in these two system are 0.89 and 0.81, respectively, which are still close to $n = 1$ reflecting approximate Einstein diffusion. Thus, the Einstein diffusion model is assumed to be appropriate to use to calculate diffusion coefficients in this study. The slope of the plot of MSD verses

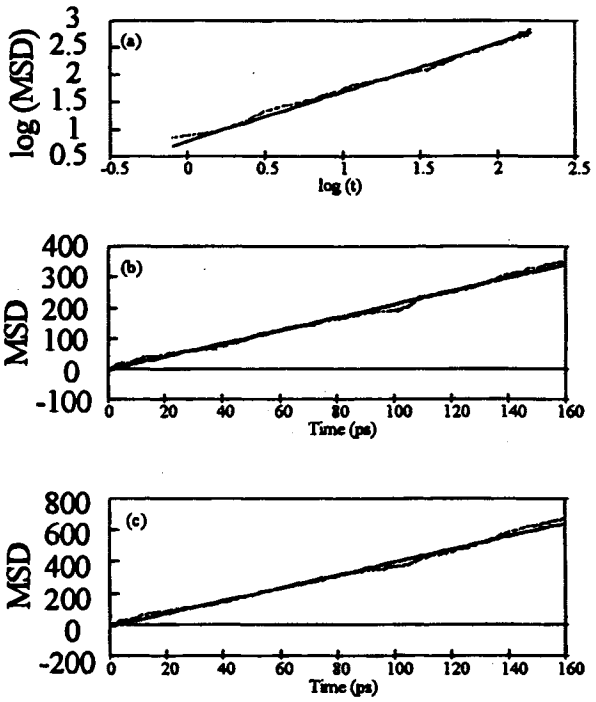

Fig. 4. MSD verses time for methanol in a DMPC bilayer at position 1. (a) log (MSD) verse log (t). (b) calculated using the z direction coordinates. (c) Calculated using the x, y, z direction coordinates.

time can, in fact, be used to calculate the diffusion coefficient. Figures 4b and 4c are sample plots of MSD verses time for all systems considered in the diffusion studies. The diffusion coefficients for methanol and propanol in a DMPC bilayer are listed in Table II. The diffusion coefficients, $D(x)$, $D(y)$, and $D(z)$, for the x, y, and z directions (z is the bilayer normal, x, y are perpendicular to z and to each other) were also calculated for comparison. The permeability constants only depend upon the diffusion rate perpendicular to the membrane, that is, the z direction.

Experimental measurements give the diffusion coefficient of methanol as 3.89×10^{-7} cm^2/s (37). The experimental measurement diffusion coefficient of propanol is 7.88×10^{-8} cm^2/s (37). The diffusion coefficient constants of methanol and propanol in a DMPC bilayer as calculated by MD simulations are 1×10^{-7} cm^2/s and 6×10^{-8} cm^2/s, respectively. The MD simulation results thus agree quite well with the experimental measurements.

Table I. The Value of n Realized from Plots of Log (MSD) Verses Log (t) for all Simulation Systems Considered

System Name	Position[a]	n
Methanol in a DMPC Bilayer	1	0.94
	2	0.93
	3	0.89
	4	0.98
Propanol in a DMPC Bilayer	1	0.91
	2	0.81
	3	0.94
	4	0.97

[a]The positions are defined in Fig. 2.

Table II. Diffusion Coefficients of Methanol and Propanol in a DMPC Bilayer

Methanol and Propanol in a DMPC Bilayer at Position	D × 10^7 cm^2/s		$D(Z)$ × 10^7 cm^2/s		$D(X)$ × 10^7 cm^2/s		$D(Y)$ × 10^7 cm^2/s	
	(M)[a]	(P)	(M)	(P)	(M)	(P)	(M)	(P)
1	1.02	0.58	1.07	0.53	1.00	0.62	1.01	0.62
2	0.67	0.49	0.71	0.43	0.69	0.42	0.62	0.54
3	0.83	0.55	0.89	0.61	0.80	0.45	0.83	0.55
4	0.71	0.60	0.68	0.65	0.74	0.57	0.68	0.57

[a]M and P indicate in methanol and propanol, respectively.

Diffusion Trajectories

In order to explore the details of the diffusion processes of methanol and propanol, time-space plots (xz plane and yz plane, where z is the bilayer normal direction) of the center mass coordinates of each of the solutes were made. Figures 5a and 5b show methanol diffusion starting ($t = 0$) at position 1. Figure 5a provides diffusion trajectory information relative to the xz plane, and Figure 5b provides diffusion trajectory information relative to the yz plane. The large trajectory ranges (about 25 Å—x direction, 30 Å—y direction,) indicate methanol diffuses over a relatively large cross-sectional area of the membrane.

Methanol could pass through the lipid bilayer center from the acyl chains of the phospholipids in one monolayer to the layer of hydrocarbon chains of the phospholipids in the other monolayer, and then diffuse back. However, when methanol enters into the hydrocarbon core, it continues to diffuse through the hydrocarbon matrix without any indication of possible back migration at the length of the simulation.

To find the diffusion trajectory in the z direction, a plot of the center mass coordinate of the solute verses time was made and is shown in Fig. 5c. The z coordinate at 25 Å, for purpose of reference, is defined as an upper bound and −25 Å as a lower bound for the corresponding hydrocarbon chain in the phospholipid. This region can be divided into three subregions based upon the torsion angle order parameter values discussed in our previous paper (34). One important observation from Fig. 5c is that methanol diffuses through the hydrocarbon chain matrix with different diffusion rates at different locations along the hydrocarbon chains of the phospholipids. Methanol passes through subregions one and two (with relatively rigid hydrocarbon chains) at rather slow rates. It passes through subregion three (with more flexible hydrocarbon chains) at a very high diffusion rate as compared to subregions one and two. The solute molecule slows down once again when it enters subregion 2 of the other monolayer. This anisotropic transport behavior further confirms that the varying extent of time-average conformational order over the hydrocarbon chain length affects the diffusion rate of a solute molecule. Solute molecules in different subregions of a hydrocarbon chain matrix appear to encounter different transport environments and use different mechanisms to pass through the respective regions. The same pattern of diffusion behavior is also observed for propanol.

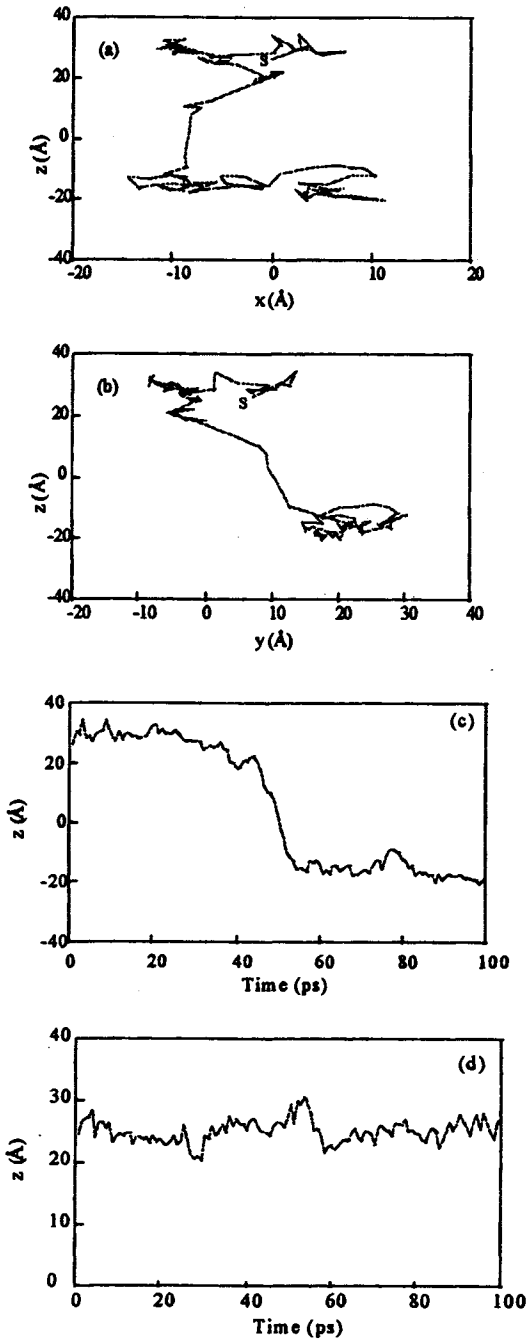

Fig. 5. Spatial projections of diffusion MD trajectories of a methanol molecule. (a) Projection in the *xz* plane. (b) Projection in the *yz* plane. (c) Methanol diffusion trajectory along the *z* direction (through the bilayer). (d) Methanol diffusion trajectory along the *z* direction using starting position 2.

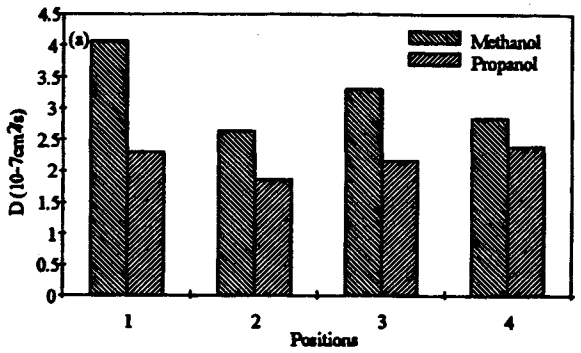

Fig. 6. The effect of solute size on diffusion rate: Diffusion coefficients of methanol and propanol in a DMPC bilayer.

Solute Size and Diffusion Rate

Since the MD simulation conditions are exactly the same for methanol and propanol, the only difference between the simulation experiments is the size of the two solute molecules. Propanol has a larger van der Waals volume. Thus, it has slower diffusion rates as compared to methanol which is as expected by intuition. It is of interest to see that the solute size factor does not exhibit the same influence over the *z*-dimension (membrane thickness) of the diffusion process. Solute size has different weights on diffusion rates in different regions of the phospholipid acyl chains. As shown in Fig. 6, there is a 43% decrease in the diffusion rate of propanol at position 1, as compared to the 19% decrease at position 4 relative to methanol. The decrease in diffusion rate appears to have a linear relationship with position. Regression analysis shows the square of the correlation coefficient, R^2, is 0.74 for the decrease in the diffusion rate of propanol as compared to the diffusion rate of methanol for the same starting position in the MD simulations. The diffusion rates of methanol, for each starting position, are used as the relative standards to calculate the percentage comparisons between the two sets of diffusion rates.

It is not difficult to conceptually understand the impact of solute size on diffusion rate in the different subregions. The torsion angle order parameters and the dynamic structural features indicate that the relative membrane density along the length of an acyl chain of a phospholipid varies. In the region close to the glycerol moiety there is high chain order. The free volume density is small. Solute size is quite critical to diffusion in this subregion. In the subregion at the end of the acyl chains there is large free volume density. Small solute molecule can move almost freely in all directions. Therefore, the size (volume) of any small molecule, such as methanol and propanol, is not as critical to diffusion rate as in regions 1 and 2. Thus, the relatively small decrease in diffusion rate is understandable.

Marrink and Berendsen (21) have reported that waters become bound to charged interfacial lipid atoms in their MD simulations. A similar type of "binding" also happens to the methanol molecule in the simulations reported here when methanol is located at the second starting position, which is also near the charge interface. It does not move from this site for the length of the simulation. This can be seen from the methanol *z*-projection trajectory shown in Fig. 5d.

A Proposed Three Zone Diffusion Model for Small Molecule Transport through a Biological Membrane

Based on the results of this study, and other experimental and theoretical studies discussed above, the phospholipid aliphatic chain matrix cannot be treated as a homogeneous phase with respect to dynamic behavior and solute transport. The different diffusion rates of small solutes, as they pass through different regions of the aliphatic chain matrix of a phospholipid bilayer, indicate the environmental differences which these sol-

ute molecules encounter. The variations in conformational and packing order, and other structural parameters of the phospholipids, suggest that a small molecule traverses the thickness of a membrane by different diffusion mechanisms. Based on the findings from our MD simulations, and other information reported in the literature, we propose that the phospholipid bilayer can be divided into three dynamic structure zones, shown in Fig. 1, which are characterized as, (a) the polar headgroup zone, (b) the relatively tight hydrocarbon chain zone (the region from torsion angle 1 to torsion angle 8), and, (c) the relatively large free volume zone around the end of an aliphatic chain. The specific molecular transport mechanisms of solute molecules at play in each of these zones are different from one another. A three zone diffusion model of molecular transport is correspondingly proposed to explain solute molecule diffusion through a lipid membrane.

In zone one, which includes the polar headgroup structures, a lateral expansion of the bilayer introduces a free volume in the phospholipid surface "lattice". However, our simulation study does not provide direct evidence for this expansion. Small molecules such as N_2 and O_2 can enter into this space. Molecules like water may get extra "help" by forming hydrogen bonds with the headgroups.

In zone two hydrocarbon chain conformational order is relatively high. The size and density of free volume sites are both relatively small. Solute molecules diffuse through this region most likely by the kink shift mechanism. The natural occurrence of kinks create structural defects where small molecules can reside. The shifting kinks along the chains move small solutes from zone two to zone three.

In zone three hydrocarbon chain conformational order is relatively low. The phospholipid atoms undergo relatively large fluctuations which generate relatively large free volume elements in both size and density. Therefore, the free volume diffusion model holds in this zone. Solute molecules can make rapid movements by jumping from one free volume cavity to another cavity. Both methanol and propanol quickly pass through the middle of a bilayer in the simulation studies reported here and, therefore, support this mechanism. Small solute molecules exhibit near isotropic motion in the middle of the lipid bilayer in the MD simulations reported here, presumably due to the large free volume present in this part of the bilayer.

Zone 2 and zone 3 in the "three zone model" correspond to regions 3 and 4 in the Marrink-Berendsen "Four Region Model". However, the boundaries in both models are approximate. The Marrink-Berendsen model has two regions to classify behavior near the headgroups. Still, Marrink and Berendsen point out that the headgroup region is the least important with respect to the permeation process.

DISCUSSION

These simulations show that kink shifts are natural occurrences in a phospholipid bilayer. The kink shifts along the lengths of the chains help transport solutes through phospholipid bilayers. The rate of kink shift propagation along the chain calculated from these MD simulations is about 2.6×10^3 cm/s. Overall, these MD simulation studies support the water transport model proposed by Träuble in 1971.

The diffusion coefficients of methanol and propanol in a lipid bilayer, as calculated from the MD simulations, also agree with experimental measurements. Both methanol and propanol show different diffusion rates in different regions of the hydrocarbon chain matrix of the lipid bilayer. The diffusion rate in the region with high torsion angle order parameters is slower than that in the region with low torsion angle order parameters. The solute size factor has more impact on the diffusion rates in the region with high torsion angle order parameters, as compared to the region with low torsion angle order parameters. Methanol moves more slowly in the region with higher torsion angle order parameters, and quickly passes through the region with low torsion angle order parameters. This behavior suggests that different diffusion mechanisms are at play in each region. The kink shift diffusion mechanism more likely occurs in the region with high torsion angle order parameters, and the free volume transport mechanism is more probable in the region with low torsion angle order parameters. It is clear that the lipid bilayer cannot be treated as a homogeneous phase with respect to solute transport since the diffusion environment at different regions along the length of the aliphatic chains is quite different in a dynamic structure.

ACKNOWLEDGMENTS

Resources of the Laboratory of Molecular Modeling and Design were used in this study. We appreciate the helpful discussions with D. Doherty of Silicon Graphics Inc. and the aid of M. Ravi and D. Singh formerly of our laboratory. Figure 3 was prepared using DataScopeLCsi2.3.0 from the National Center for Supercomputer Applications at the University of Illinois at Urbana-Champaign.

REFERENCES

1. W. Y. Kuu, R. W. Wood, and T. Roseman. In A. Kydonieus (ed.), *Treatise on Controlled Drug Delivery*, Marcel Dekker, Inc., New York, pp. 37–147 (1992).
2. A. Finkelstein. *Water Movement through Lipid Bilayers, Pores, and Plasma Membranes*, John Wiley and Sons, New York (1987).
3. T. Hanai and D. A. Haydon. *J. Theor. Biol.* **11**:370–382 (1966).
4. J. B. Reeves and R. M. Dowben. *J. Memb. Biol.* **3**:123–141 (1970).
5. A. Carruthers and D. L. Melchior. *Biochemistry* **22**:5797–5807 (1983).
6. D. W. Deamer and J. Bramhall. *Chem. Phys. Lipids* **40**:167–175 (1986).
7. J. C. Weaver, K. T. Powell, R. A. Mintzer, S. R. Sloan, and H. Ling. *Bioelectrochem. Bioenerg.* **12**:405-12 (1984).
8. W. R. Lieb and W. D. Stein. *Nature (London).* **224**:240–243 (1969).
9. J. M. Wolosin, H. Ginsburg, W. R. Lieb, and W. D. Stein. *J. Gen. Physiol.* **71**:93–100 (1978).
10. W. D. Stein. In S. L. Bonting and J. J. H. H. M. de Pont (eds), *Membrane Transport*, Elsevier/North-Holland Biomedical., New York, pp. 1–28 (1981).
11. R. O., Potts and M. L. Francoeur. *Natl. Acad. Sci. U.S.A.* **87**:3871–3873 (1990).
12. H. Träuble. *J. Memb. Biol.* **4**:193–208 (1971).
13. T. H. Haines and L. S. Liebovitch. In E. A. Dissolve and S. A. Simon (eds), *Permeability and Stability of Lipid Bilayers*, CRC Press, Boca Raton, FL, pp. 123–136 (1995).
14. J. Day and C. R. Willis. *J. Theor. Biol.* **94**:367–390 (1982).
15. J. F. Nagle and H. L. Scott. *Biochim. Biophys. Acta.* **513**:236–243 (1978).
16. S. Marcelja. *Biochim. Biophys. Acta.* **367**:165–176 (1974).
17. R. Kjellander and S. Marcelja. *Chem. Phys. Lett.* **120**:393–396 (1985).

18. S. J. McKinnon, S. L., Whittenburg, and B. Brooks. *J. Phys. Chem.* **96**:10497–10506 (1992).
19. D. Bassolino-Klimas, H. E. Alper, and T. R. Stouch. *J. Am. Chem. Soc.* **117**:4118–4129 (1995).
20. D. Bassolino-Klimas, H. E. Alper, and T. R. Stouch. *Biochemistry* **32**:12624–12637 (1993).
21. S. Marrink, and H. J. Berendsen. *J. Phys. Chem.* **98**:4155–4168 (1994).
22. R. A. Pearlstein. CHEMLAB-II Users Guide, CHEMLAB Inc., 1780 Wilson Dr., Lake Forest, IL 60045, 1988.
23. N. L. Allinger and Y. H. Yuh. Operating instruction for MM2 and MMP2 Program—1977 Force Field. *Quantum Chemistry Program Exchange*. Chemistry Department, Indiana University, 1980.
24. A. J. Hopfinger and R. A. Pearlstein. *J. Comput. Chem.* **5**:486–499 (1984).
25. L. Radom, W. J. Hehre, and J. H. Pople. *J. Am. Chem. Soc.* **94**:2371–2381 (1972).
26. T. R. Stouch, K. B. Ward, A. Altiei, and A. T. Hagler. *J. Comp. Chem.* **12**:1033–1046 (1991).
27. H. Hauser, I. Pascher, R. H. Pearson, and S. Sundell. *Biochim. Biophys. Acta.* **650**:21–51 (1981).
28. M. Suwalsky. In C. Hidalgo (ed), *Physical Properties of Biological Membranes and Their Functional Implications*, New York, Plenum Press, pp. 1–20 (1988).
29. D. C. Doherty. MOLSIM User Guide. The Chem21 Group, 1780 Wilson Dr., Lake Forest, IL 60045 (1994).
30. Cerius^2: Molecular Simulation Incorporated. 16 New England Executive Park, Burlington, Massachusetts, 01803-5297. USA.
31. DataScopeLS2.0.3, The National Center for Supercomputer Applications at the University of Illinois at Urbana-Champaign, 1993.
32. T. Xiang. *Biophys. J.* **65**:1108–1120 (1993).
33. E. Egberts, S. J. Marrink, and H. J. C. Berendsen. *Eur. Biophys. J.* **22**:423–436 (1994).
34. B. Jin, and A. J. Hopfinger. Characterization of lipid membrane dynamics by simulation: 2. Quantitative determination of lipid fluidity, 1996a *Computational Polym. Sci.*, in press.
35. B. Jin, and A. J. Hopfinger. Characterization of lipid membrane dynamics by simulation: 1. Torsion angle motions of the linear chains. 1996b. *Biopolymers*, in press.
36. B. Jin. Intramolecular and intermolecular modeling, Ph.D. Dissertation. 1996c.
37. W. D. Stein. *Transport and Diffusion across Cell Membranes*. Academic Press, Inc., New York, 1986.